doi: 10.82124/CEAS-GNC-2026-066 CEAS-GNC-2026-066

Thruster Pointing Mechanism Control for HENON Deep Space Transfer

Michele Olmo AOCS Engineer, Argotec s.r.l, Turin, Italy. michele.olmo@argotecgroup.com

Giorgio Saita AOCS Engineer, Argotec s.r.l, Turin, Italy. giorgio.saita@argotecgroup.com

Nicolò Benigno AOCS Engineer, Argotec s.r.l, Turin, Italy. nicolo.benigno@argotecgroup.com

Davide Calcagno System Engineer, Argotec s.r.l, Turin, Italy. davide.calcagno@argotecgroup.com

Alessandro Lovesio SW Engineer, Argotec s.r.l, Turin, Italy. alessandro.lovesio@argotecgroup.com

Alessandro Vitiello Mission Analyst, Argotec s.r.l, Turin, Italy. alessandro.vitiello@argotecgroup.com

Davide Monferrini Project Manager, Argotec s.r.l, Turin, Italy. davide.monferrini@argotecgroup.com

Luigi Guarino Project Manager, Argotec s.r.l, Turin, Italy. luigi.guarino@argotecgroup.com

ABSTRACT

This paper presents the Thruster Pointing Mechanism (TPM) control strategy developed by Argotec in the context of the ESA CubeSat mission HENON. The mission is led by Argotec and it is developed by a consortium composed by INAF, as principal investigator, University of Calabria, University of Florence, SPACEDYS, Imperial College, ASRO and IMT. An external contribution is provided by Charles University and Mars Space Limited for the payload suite and the Electrical Propulsion System. The mission aims at studying space weather phenomena and HENON will be the first CubeSat to reach a Distant Retrograde Orbit (DRO) to achieve this goal. The spacecraft will perform a deep space transfer to the DRO by means of a gridded ion-thruster, providing low thrust and high specific impulse. The uncertainties on the knowledge of the Center of Mass (CoM) position required a gimbal to orient the thrust along the CoM direction, in order to avoid the generation of parasitic torques due to the propulsion system. However, the uncertainties on the thrust vector direction, due to the TPM accuracy and the electric thruster's grids misalignments, generate a residual parasitic torque on the spacecraft. This disturbance would negate the spacecraft the possibility to perform the deep space transfer, therefore a TPM control strategy is developed to exploit the gimbal to generate torques counteracting the residual parasitic momentum build-up. This paper demonstrates the effectiveness of the proposed strategy in reducing the parasitic angular momentum build-up and its easiness of adaption to scenarios involving different errors and control intervals.

Keywords: Thruster Pointing Mechanism, Angular Momentum Management, Residual Parasitic Torque, Electric Propulsion, Deep Space

Nomenclature

ADCS = Attitude Determination and Control System
AOCS = Attitude and Orbit Control System
CEPS = CubeSat Electric Propulsion System
CoM = Center of Mass
CPS = CubeSat Propulsion System
CSS = Coarse Sun Sensor
DRO = Distant Retrograde Orbit
FCA = Faraday Cup Analyser
FoV = Field of View
MAGIC = Magnetometer from Imperial College
MRCS = Micro-Reaction Control System
MSL = Mars Space Limited
REPE = Relativistic Electron and Proton Experiment
RW = Reaction Wheel
S/C = Spacecraft
ST = Star Tracker
TPM = Thruster Pointing Mechanism
TPME = Thruster Pointing Mechanism Electronics

1 Introduction

1.1 HENON Mission

The HENON mission springs from the unanimously recognized and urgent need of making significant advances in the Space Weather field. For the fulfilment of the mentioned need, two of the most important elements are:

- To realize a quality leap in the capabilities to predict Space Weather effects.
- To understand the Space Weather physical mechanisms.

The first element pertains to a question that requires efficient answers from an operational point of view. The second element pertains to the understanding of basic processes of plasma physics at the base of the Space Weather that will help in improving our capabilities of monitoring Space Weather hazards. The physical processes that occur on the Sun and in space allow the acceleration of particles up to relativistic energies and the explosive release of energy that disrupt the physical state of interplanetary and planetary space environments. In particular, disturbance conditions in circumterrestrial space have a negative impact on human life, which affects essential technological systems and human health itself. Such direct and potentially dangerous consequences on our society led to significant investment, at national and international level, to advance the forecasting capabilities of the Space Weather conditions and disturbances.

The mission goal is to perform a demonstration of Space Weather measurements in a Distant Retrograde Orbit (DRO), allowing for real-time warnings of solar storms (sunward side) up to 3 hours before they reach Earth. The mission will also be a demonstration of deep space CubeSat technologies, such as the electric propulsion system enabling the transfer from Sun-Earth L1/L2 to the target DRO.

The HENON mission is a technology demonstrator, acting as a pathfinder for advanced space weather services. Based on the key outcome and achievements of this mission, a constellation is foreseen by ESA to guarantee a complete coverage and service continuity [1].

1.2 Technical Challenges

As previously mentioned, HENON will perform a transfer in deep space by means of its electric propulsion system to reach the DRO. Despite the increasingly high number of CubeSats that are being launched, only a small percentage of them target deep space orbits [2]. Performing a deep space transfer exploiting its own propulsion system contributes to make HENON even more unique. The transfer phase is characterized by firing arcs that shall provide up to 6 days of uninterrupted thrust. However, the electric propulsion system brings with it two sources of thrust vector errors:

- the TPM accuracy: affecting both the thrust vector direction and point of application.
- the ion-thruster grids misalignments: affecting the thrust vector direction and introducing a swirl torque component as well.

These errors generate residual parasitic torques even when the TPM is commanded to align the thrust vector along the CoM direction. The residual parasitic torques cause the RWs to store residual parasitic momentum. As presented in the following sections, the effect of the residual parasitic torques causes the RWs to exceed their saturation limit, hindering the spacecraft's ability to properly complete a firing arc.

The momentum management through gimbaled thrusters has been studied in [3] and [4]. In [3] it is proposed an approach to generate torques with an electric propulsion thruster in order to mitigate the Solar Radiation Pressure (SRP) disturbance on the spacecraft. This condition is different than HENON's, where the major source of disturbance is the propulsion system itself. The errors introduced by the TPM pointing accuracy and the grids misalignments are one order of magnitude greater than those introduced by the environment. In [4], the case study M-Argo mission considers a scenario more similar to HENON. However, HENON TPM control strategy is intended to minimize the implementation effort on the OBC as well. HENON proposed pointing strategy is then later described in Section 3.

2 HENON CubeSat

HENON is a 12U XL CubeSat equipped with a payload suite consisting of state-of-the-art, miniaturised space weather instrumentation tailored for detecting heliospheric disturbances several hours in advance of arrival at Earth [1]. The selected payload suite, shown in Figure 1, includes:

- MAGIC (Magnetometer from Imperial College), developed by Imperial College London (UK), under ESA GSTP programme.
- REPE (Relativistic Electron and Proton Experiment), developed by ASRO/University of Turku (FI), under ESA GSTP programme.
- FCA (Faraday Cup Analyser), developed by Charles University (CZ), under ESA PRODEX programme.

To perform the deep space transfer HENON is equipped with an electric propulsion system as later described in Section 2.2

2.1 HENON Reference Frame

In Figure 1 it is shown the Spacecraft (S/C) body reference frame. It has the following properties:

- Origin set at the geometrical centre of the plate that contains the CubeSat Electric Propulsion System (CEPS) thruster head.
- $+Z_{body}$ axis aligned with the CEPS thruster axis. Positive direction towards the payloads' face.
- $+X_{body}$ axis perpendicular to the High-Gain antenna FoV. Positive direction towards the High-Gain antenna.
- $+Y_{body}$ aligned with the solar panels rotation axis, forming a right-handed frame.

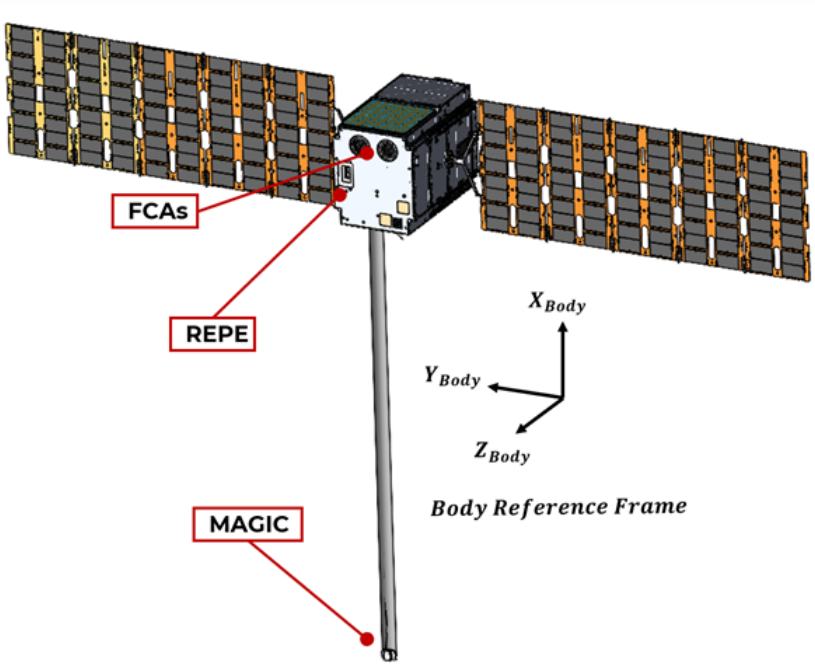

Fig. 1 HENON Body Reference Frame

2.2 HENON AOCS Suite

HENON Attitude and Orbit Control System (AOCS) suite is constituted of two main subsystems:

- **ADCS**: The baseline Attitude Determination and Control System (ADCS) for HENON is an integrated solution based on a central avionics box which include a Star Tracker (ST) and Gyroscopes. The avionic box is paired with a set of external Reaction Wheels (RWs) and Coarse Sun Sensors (CSSs).
- **CPS**: The CubeSat Propulsion System (CPS) is made of two main units: the CubeSat Electric Propulsion System (CEPS), used to perform the interplanetary transfer phase up to the target orbit and the micro-Reaction Control System (mRCS), used to perform momentum dumping. The entire module is developed by a consortium led by Mars Space Limited (MSL) under ESA GSTP [5]. In particular, MSL is also responsible for the thruster manufacturing, while AVS UK is responsible for TPM manufacturing.

The overall architecture AOCS suite architecture is reported in Figure 2.

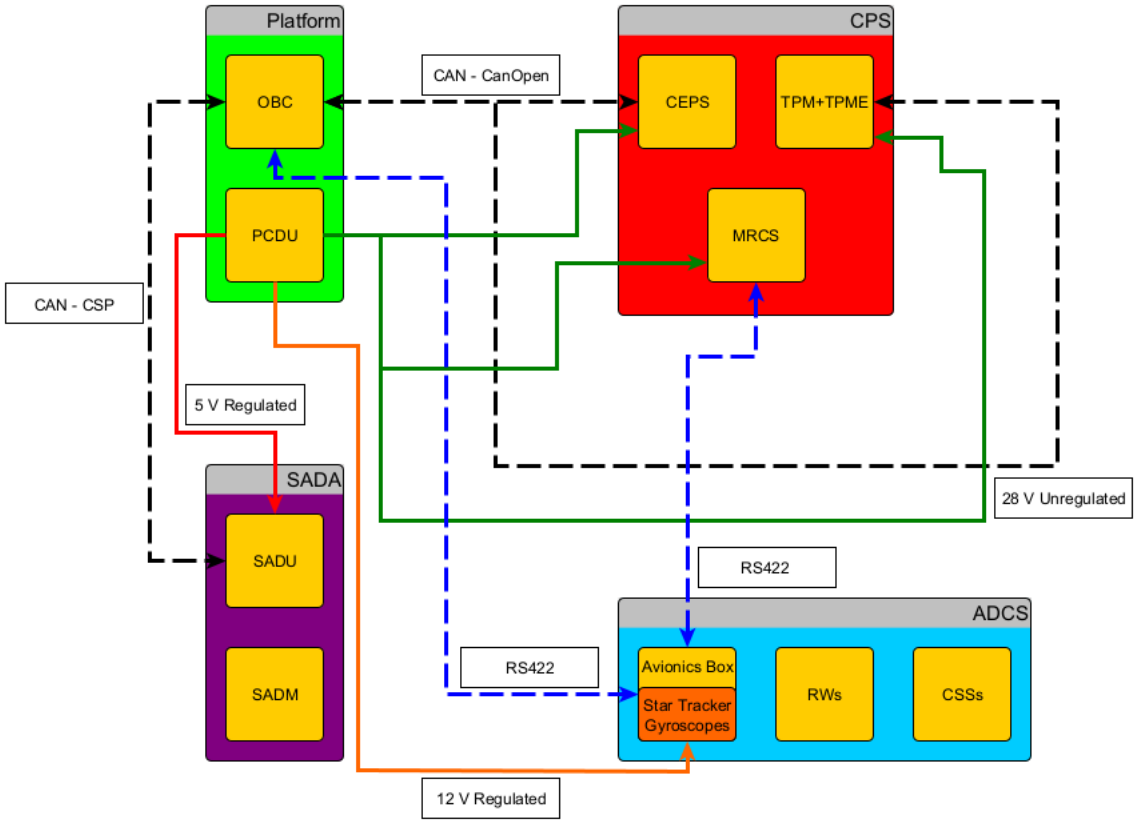

Fig. 2 HENON AOCS Architecture

2.2.1 RWs Configuration

HENON mounts a set of 4 RWs in the following configuration:

- 3 RWs mounted with rotation axes parallel to the body axes.
- 1 RW tilted with respect to the other body axes.

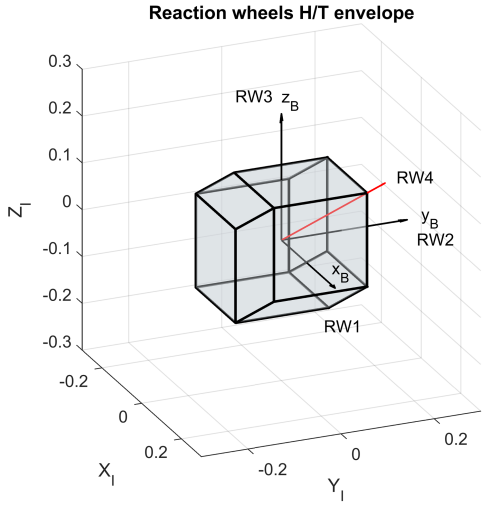

Fig. 3 HENON RWs Configuration

HENON RWs configuration and angular momentum envelope are depicted in Figure 3. RWs 1-to-3 have a $0.1 Nms$ momentum storage capacity, while RW4 has a $0.05 Nms$ momentum storage capacity.

3 TPM Model and Control

In this section it is described the model and results of the CEPS residual parasitic torques analysis. The TPM is used to orient the thrust vector along the CoM direction, however there are errors and uncertainties preventing an ideal alignment. The resulting misalignment generates what in this paper are called “residual parasitic torques”. The sources of this phenomenon are:

- TPM accuracy
- Ion-thruster grids misalignments

3.1 TPM Control Algorithm

In this section it is presented a strategy that can be implemented either on-board or from ground. In the context of an on-ground implementation, the TPM position update would be calculated and commanded from ground during the coasting arcs separating one firing arc from the next one. On the other hand, an on-board implementation allows to increase the number of TPM position updates. In this scenario, the OBC would autonomously perform the calculation and position updates after a fixed time interval. In this paper, analyses involving one position update per day are presented. This proposed approach allows to reduce the propellant required to perform desaturation manoeuvres during the mission.

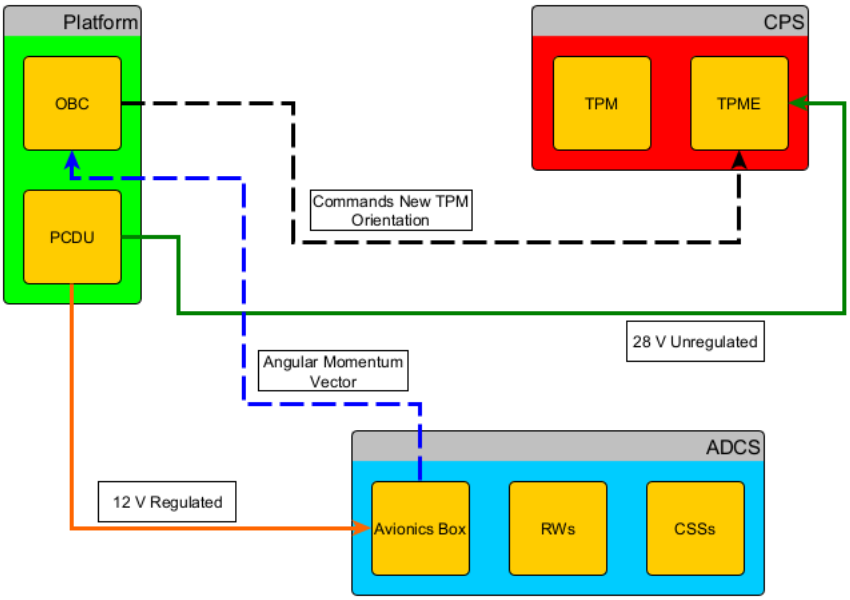

Fig. 4 HENON TPM Control Loop

The TPM control strategy shown in Figure 4 is structured as follows:

- During a firing arc the CEPS is turned off at regular intervals. Throttling to a lower thrust level could be an alternative option.
- After turning off the CEPS, the ADCS provides the 3-axes angular momentum distribution. The following algorithm is run:
  - Based on the measurement of the angular momentum of the ADCS, and on the control interval t_{corr}, the corrective torque T_{corr} is computed.
  - The cost function $\mathcal{L} = 10^6||T_{x,corr} - T_x(\delta,\eta)|| + 10^6||T_{y,corr} - T_y(\delta,\eta)|| + 10^4||T_{z,corr} - T_z(\delta,\eta)||$ is minimized via particle swarm optimization [6] to determine the angles δ and η to command to the TPME in order to obtain the requested corrective torque.
- After the TPM is correctly reoriented, the CEPS is turned on again (or throttled to a higher thrust level) and the firing arc is resumed.

The choice of using particle swarm optimization in this context is driven by two factors:

- no gradient computation is needed;
- no initial guess is required.

The particles initial position and velocity proved to have a negligible effect on the optimizer output.

3.2 Mathematical Model

The mathematical model is based on the following notation and assumptions:

- All vectors expressed in body reference frame coordinates. Vectors are indicated in bold.
- S/C CoM position vector: $\mathbf{r_{CoM}}$.
- Thruster head exit position vector: $\mathbf{r_{TH}}$.
- Thrust vector aligned with thruster head axis in ideal conditions (no mounting or grids misalignment errors).
- Reference thrust level: $F_0 = 1.7mN$.
- Thrust vector applied at the exit of the thruster head.
- Swirl torque model: $\mathbf{T_{swirl}} = 0.12 \cdot 10^{-6} \frac{F_0}{2.2} \begin{bmatrix} 0 \\ 0 \\ 1 \end{bmatrix} Nm$ (F_0 in mN).

The residual parasitic torques are computed as cross-product of the position vector of the thrust vector point of application (with respect to the CoM) and the thrust vector itself.

$$\mathbf{T_{res}} = \mathbf{r} \times \mathbf{F} + \mathbf{T_{swirl}} \tag{1}$$

From Equation 1 it is possible to notice that in the ideal case the position vector of the thrust point of application will be aligned to the CoM direction and the thrust vector will be parallel to it as well. This means that the only contribution to the residual parasitic torques is due to the swirl torque. When an error is introduced, the alignment can not be achieved and an additional torque contribution is generated.

3.2.1 Thruster Head Alignment with the S/C CoM

The thuster head exit rest position is aligned with the $-Z_{body}$ axis of the spacecraft. To compute the coordinates of the thruster head exit when it is aligned with the CoM, the following calculation is carried on.
The Euler axis and angle mapping the rotation of the Z_{body} axis to the CoM position vector direction are computed as

$$\mathbf{a} = \mathbf{Z_{body}} \times \mathbf{r_{CoM}} \Rightarrow \hat{\mathbf{a}} = \frac{\mathbf{a}}{||\mathbf{a}||} \tag{2}$$

$$\alpha = arccos(\mathbf{Z_{body}} \cdot \hat{\mathbf{r}}_{\mathbf{CoM}}) \tag{3}$$

The corresponding rotation matrix is derived as

$$\mathbf{R_{TPM}} = \mathbf{I} \cdot cos(\alpha) + \hat{\mathbf{a}}_{\times} sin(\alpha) + [1 - cos(\alpha)](\hat{\mathbf{a}} \times \hat{\mathbf{a}}) \tag{4}$$

The position vector of the thruster head exit and the thrust vector then are

$$\mathbf{r_{TH}}^1 = \mathbf{R_{TPM}} \cdot \mathbf{r_{TH}}^0 \tag{5}$$

$$\mathbf{F}^1 = \mathbf{R_{TPM}} \cdot \mathbf{F}^0 \tag{6}$$

The rest position of the thruster head and the associated thrust vector are identified by superscript 0. When a rotation is applied to point the thrust vector towards the CoM, the resulting vectors are identified by superscript 1.

3.2.2 Introduction of TPM Error

To apply the TPM accuracy error it is first computed the deviation of the vectors from the Z_{body} axis reference direction. Then the same rotation matrix computed in Equation 4 is used to obtain the rotated vectors. The deviated vectors are computed by means of the angles δ and η shown in Figure 5.

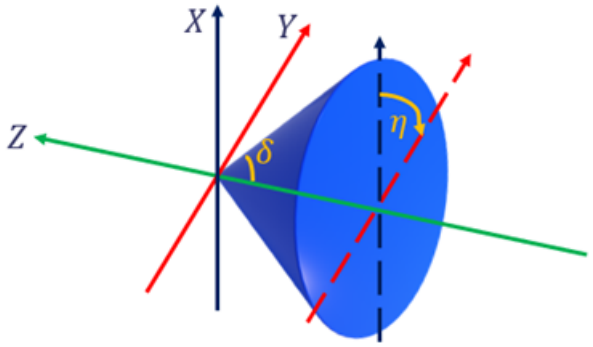

Fig. 5 δ and η Parametric Angles

The thruster head vector and the thrust vectors after the application of TPM error are computed as:

$$\mathbf{r_{TH}}^{1,dev} = ||\mathbf{r_{TH}}^1|| \begin{bmatrix} -sin(\delta)cos(\eta) \\ -sin(\delta)sin(\eta) \\ -cos(\delta) \end{bmatrix} \Rightarrow \mathbf{r_{TH}}^2 = \mathbf{R_{TPM}} \cdot \mathbf{r_{TH}}^1 \tag{7}$$

$$\mathbf{F}^{1,dev} = ||\mathbf{F}^1|| \begin{bmatrix} sin(\delta)cos(\eta) \\ sin(\delta)sin(\eta) \\ cos(\delta) \end{bmatrix} \Rightarrow \mathbf{F}^2 = \mathbf{R_{TPM}} \cdot \mathbf{F}^1 \tag{8}$$

The thruster head vector and thrust vector deviation from the rest position are identified by means of the superscript 1,dev. The deviated vectors are then rotated by means of $\mathbf{R_{TPM}}$. This allows to obtain the vectors components when pointing towards the CoM and affected by the TPM accuracy errors. These vectors are identified by the superscript 2.

3.2.3 Introduction of Grids Misalignment Error

It is assumed that this error only affects the thrust vector and not the thruster head vector. The computation of the rotated thrust vector is carried out in an analogous fashion as the above steps. Euler axis and angle are computed as:

$$\mathbf{a} = \mathbf{Z_{body}} \times \mathbf{F}^2 \Rightarrow \hat{\mathbf{a}} = \frac{\mathbf{a}}{||\mathbf{a}||} \tag{9}$$

$$\alpha = arccos(\mathbf{Z_{body}} \cdot \hat{\mathbf{F}}^2) \tag{10}$$

4 Montecarlo Analyses Results

Given the random nature of the errors affecting the thrust vector, Montecarlo analyses are performed in order to assess the probability of exceeding the RWs momentum threshold during a firing arc. The δ angles are introduced as a zero-mean Gaussian distribution and it defines the error cone half-cone angle. On the other hand, the η angle identifies a unique angular position on a cone of aperture δ. The η angles are modeled under the assumption of rotational simmetry around the cone axis and follow a uniform distribution. The results are presented in the following sections.

4.1 No-TPM Control Montecarlo Analysis

HENON foresees nominal 6 days long firing arcs to be performed during its transfer phase. Figure 6 shows the angular momentum accumulated at the end of a firing arc due to the residual parasitic torques. Each sample of the Montecarlo analisys is run from zero initial angular momentum and varying the TPM and grids errors between samples.

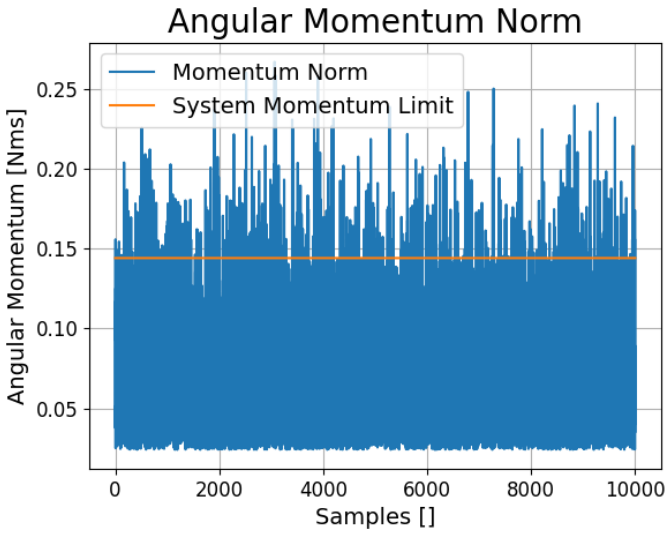

Fig. 6 Uncontrolled Momentum Build-up

If the RWs saturation threshold is reached, the firing arc can not be completed without performing desaturation maneuvers. However, this would require frequent autonomous desaturations, increasing the system complexity. In addition, the angular momentum stored in this condition would require more propellant than what is available. Given that about 49% of the samples exceed the RWs saturation threshold, the TPM is used to orient the thruster in such a way that a corrective torque is generated, reducing the overall system momentum.

4.2 On-Ground TPM Control Montecarlo Analysis

To manage the momentum build-up, it is first investigated a strategy that is implementable on-ground. This would be achieved by reducing the firing arcs duration and adjusting the thruster position at the

end of each firing arc. This would allow for partial RWs desaturation, limiting the usage of the cold gas thrusters to save propellant. This strategy would be compatible with an on-ground control strategy, as the control angles could be computed on-ground and then sent to the spacecraft as telecommands during communication windows.

It is investigated a scenario involving firing arcs reduced to 3 days, with the thruster position adjusted at the end of each firing arc.

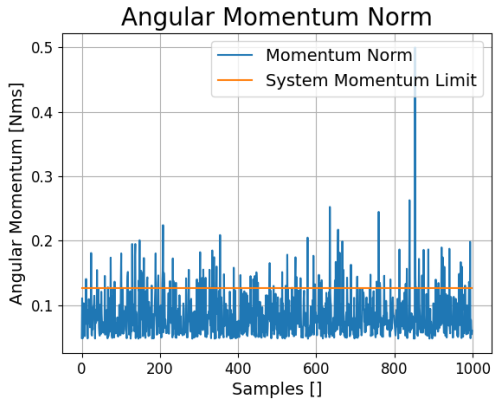

(a) On-Ground Control: Angular Momentum Norm After 6 Days

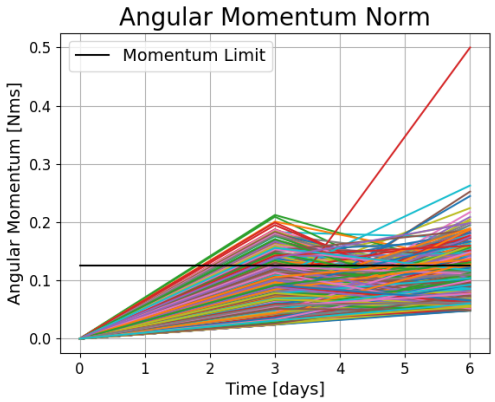

(b) On-Ground Control: Angular Momentum Build-Up Over 6 Days

Fig. 7 On-Ground Control: Angular Momentum Norm Analysis Over a 6 Days Period

In Figure 7b it is possible to notice that the momentum threshold is exceeded before 3 days in a significant number of samples. This would require for a shorter control interval, which is incompatible with an on-ground control strategy. Furthermore, Figure 7a shows that about 13% of samples exceed the saturation threshold at the end of a 6 days period. While this is a significant improvement with respect to the uncontrolled scenario, it is still not enough to grant uninterrupted firing arcs of the desired duration. An on-board control strategy is then investigated to allow for shorter control intervals.

4.3 On-Board TPM Control Montecarlo Analysis

The on-board control strategy considers fixed control intervals of 1 day per week. This choice is preferred to a continuous closed-loop solution because:

- A fixed time control interval allows for a limited number of control actions during a firing arc. This reduces the overall maneuver complexity, which is critical for a CubeSat requiring such a high level of autonomy.
- The TPM continuous movement would result in performance degradation. The accuracy will worsen with continuous movement of the mechanism. A limited number of reorienting maneuvers reduces the pointing performance degradation, maintaining the accuracy at nominal value.

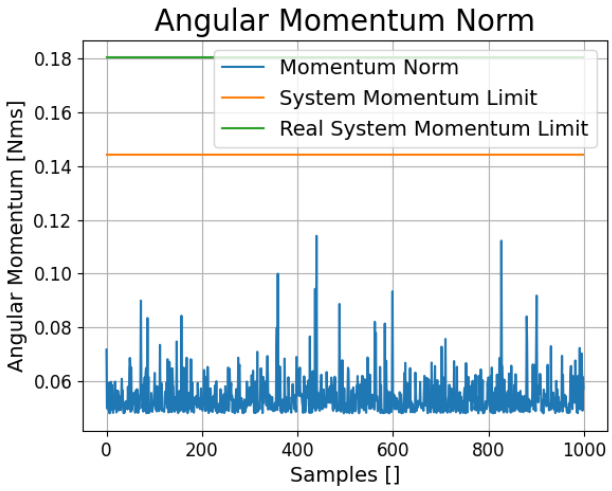

(a) On-Board Control: Angular Momentum Norm After 6 Days

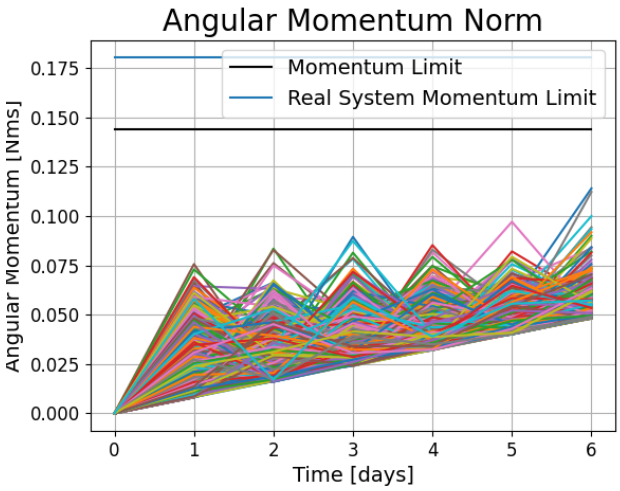

(b) On-Board Control: Angular Momentum Build-Up Over 6 Days

Fig. 8 On-Board Control: Angular Momentum Norm Analysis Over a 6 Days Period

In Figure 8 one can notice that this strategy makes it possible to never exceed the saturation threshold over a 6 days period. The implemented strategy allows to mitigate the momentum build-up. Still, it shall be noticed that it is not possible to reduce momentum build-up indefinitely. This is due to the propulsion system swirl torque that acts on the spacecraft Z_{body} axis, and thus it can not be managed by the TPM as it is directed along the thruster axis.

5 Conclusions

This paper presented the TPM control strategy developed for the HENON mission. The developed strategy consists in changing the thruster's orientation at fixed time instants in order to provide a torque on the spacecraft that dumps the residual parasitic angular momentum. The simulations carried out in this paper show that, by setting the control interval to one day, it is possible to maintain the angular momentum storage below ADCS imposed limits. By reducing the angular momentum build-up, the propellant consumption required to off-load the RWs is significantly reduced. In addition, by tuning the number of corrective actions and the control time, it is possible to manage more severe errors that would lead to an increased angular momentum build-up. This feature enhances the strategy's in-orbit reliability by allowing to manage even unforeseen sources of error.

Adjusting the thruster's position at discrete time instants allows to reduce the computational burden on the OBC, compared to a continuous time approach. This is because the spacecraft is not required to continuously monitor the agular momentum stored by the RWs, nor to continuously move the thruster, hence reducing TPM wear and performance degradation.

The proposed approach proved to be extremely effective in reducing the spacecraft angular momentum, while maintaining a relatively simple structure, resulting in an effective option to implement on a CubeSat.

Future work stemming from this study might include the possibility to introduce an adaptive control interval, based on the history of angular momentum monitoring.

Acknowledgments

The mission is led by Argotec and developed under ESA's General Support Technology Programme (GSTP) Fly Element through contract No. 4000147483/25/NL/MGu. Argotec acts as prime contractor, leading a consortium composed by INAF, as principal investigator, University of Calabria, University of Florence, SPACEDYS, Imperial College, ASRO and IMT. An external contribution is provided by Charles University and Mars Space Limited for the payload suite and the Electrical Propulsion System. HENON GSTP's funding is provided by the Italian Space Agency as part of the Italian national CubeSat program ALCOR, as well as by space agencies from the UK and Finland.

Declaration of Use of Artificial Intelligence

Artificial intelligence was not used in the work presented.

References

[1] European Space Agency. Henon mission. https://www.esa.int/Enabling_Support/Space_Engineering_Technology/Technology_CubeSats/HENON, 2025. Accessed: 30 October 2025.

[2] Erik Kulu. Cubesats & nanosatellites - 2024 statistics, forecast and reliability. In *Proceedings of the 75th International Astronautical Congress (IAC 2024)*, Milan, Italy, Oct. 2024.

[3] Riccardo Calaon, Cody Allard, Hanspeter Schaub, and Leah Kiner. Momentum management of a spacecraft equipped with a dual-gimballed electric thruster. In *Proceedings of the AAS Rocky Mountain GNC Conference*, Breckenridge, Colorado, Feb. 2023.

[4] Andrea Pizzetti, Antonio Rizza, and Francesco Topputo. Autonomous wheel off-loading strategies for deep-space cubesats. *Aerotecnica Missili e Spazio*, 2022.

[5] Stephen Clark, Francesco Guarducci, Dominic Marangone, Rhodri Lewis, Alexander J.N. Daykin-Iliopoulos, Klevis Gasa, Graham Skingle, Peter Turner, Maria Smirnova, Aloha Mingo, Phil McNutt, Joseph Kigonya, Johan Kuiper, Emilia Wegrzyn, and Neil Wallace. Development of a cubesat propulsion system. In *Proceedings of the 39th International Electric Propulsion Conference (IEPC)*, London, United Kingdom, Sept. 2025.

[6] Cornell University. Particle swarm optimization. https://optimization.cbe.cornell.edu/index.php?title=Particle_swarm_optimization, 2025. Accessed: 30 October 2025.